A New Reactive Absorption Model Using Extents of Reaction and Activities. I. Application to Alkaline-salts-CO2 Systems

Serena Delgado, Alain Gaunand, Christophe Coquelet, Renaud Cadours, Céline Volpi

A New Reactive Absorption Model Using Extents of Reaction and Activities. I. Application to Alkaline-salts-CO_2 Systems

Submitted to *Chemical Engineering Science*

Serena Delgado[a,b], Alain Gaunand[a]*, Christophe Coquelet[a,c]*, Renaud Cadours[a,b] and Céline Volpi[b]

[a] *Mines Paris, PSL University, CTP (Centre of Thermodynamics of Processes) 35 Rue Saint Honoré 77305 Fontainebleau Cedex, France*

[b] *TotalEnergies SE, Tour Coupole, 2 place Jean Millier, 92078 Paris La Défense Cedex, France*

[c] *Université de Toulouse, IMT Mines Albi, CNRS UMR 5302, Centre Rapsodee Campus Jarlard, 81013 Albi CT Cedex 9, France*

**Corresponding authors e-mail addresses: alain.gaunand@minesparis.psl.eu, christophe.coquelet@mines-albi.fr.*

Keywords

Gas-liquid absorption, Kinetic model, Non ideality, Hydroxide solutions, CO_2 absorption

Abstract

CO_2 absorption into basic aqueous solutions is widely used for CO_2 separation from gas streams (e.g., for natural gas purification). CO_2 loading and ionic strength increase significantly along industrial columns. In absorption modelling, deviation from ideality should then be considered.

This study implements a general steady-state model for reactive gas-liquid absorption. Firstly, equilibrium relations, Nernst-Planck diffusion fluxes and reaction rates are written based on activities. Secondly, local fluxes are related by stochiometric constraints through extents of reaction.

In a first case study, the model, together with an appropriate thermodynamic representation, was applied with the stagnant film theory (Whitman, 1923) to alkaline salts-water-CO_2 systems. The following Arrhenius expression was found for the direct kinetic constant of reaction $CO_2 + HO^- \leftrightarrow HCO_3^-$: $\ln (m^3.mol^{-1}.s^{-1}) = 19.84 - 5248.8/T\ (K)$ – 12% overall AAD. This kinetic law can be used in any system involving this reaction (e.g., aqueous amine solutions). This part I paves the way to the further study of CO_2 absorption into aqueous amine solutions.

Nomenclature

1	A	Logarithm of Arrhenius pre-exponential factor
2	a_i	Activity of species i (mol.m^{-3})
3	$a_{1,0}$	Activity of absorbed gas at gas-liquid interface (mol.m^{-3})
4	c_i	Molar concentration of species i (mol.m^{-3})
5	$c_{1,0}$	Concentration of absorbed gas at gas-liquid interface (mol.m^{-3})
6	$c_{abs,tot}$	Total absorptive species concentration (mol.m^{-3})
7	C_i	Normalised concentration of species i (-)
8	$c_{b,i}$	Liquid bulk concentration of species i (mol.m^{-3})
9	$c_{N,i}$	Normalisation concentration of species i (mol.m^{-3})
10	D_i	Diffusivity of species i in solution (mol.m^{-3})
11	E	Enhancement factor (-)
12	E_A	Activation energy (J.mol^{-1})
13	f_{obj}	Optimisation objective function (-)
14	G	Gibbs free energy (J)
15	H_1	Henry's constant of absorbed gas at infinite dilution (Pa)
16	Ha_j	Hatta number of reaction j (-)
17	j_i	Flux of species i through liquid film (mol.m^{-2}.s^{-1})
18	$j_{1T,0}$	Total absorption flux of absorbed gas (mol.m^{-2}.s^{-1})
19	k_j	Reaction j kinetic constant
20	K_j	Reaction j equilibrium constant
21	$K_{N,j}$	Reaction j normalising equilibrium constant
22	$k_{L,1}$	Liquid-side mass transfer coefficient regarding the absorbed gas (m.s^{-1})
23	M	Matrix of the differential problem for concentration-related equations
24	n_C	Number of solute constituents in liquid phase
25	n_i	mole number of species i (mol)
26	$n_{R,kin}$	Number of finite-rate reactions in the reaction mechanism
27	$n_{R,eq}$	Number of reactions at equilibrium in the reaction mechanism
28	o^D_{ij}	Direct kinetic order of species i in reaction j (-)
29	o^R_{ij}	Reverse kinetic order of species i in reaction j (-)
30	P	Pressure (Pa)
31	$p_{1,0}$	Pressure of absorbed gas at gas-liquid interface (Pa)
32	r_j	Reaction rate of reaction j (mol.m^{-3}.s^{-1})
33	T	Temperature (K)
34	x_i	Mole fraction of species I (-)
35	X_i	Vector of the differential problem for concentration-related equations
36	z	Distance from interface (m)
37	Z	Normalised distance from interface (z)
38	z_i	Number of charges of species I (-)
39	Z_{Di}	Diffusion-concentration ratio of species i (-)
40	*Constants*	
41	$\mathcal{F}$	Faraday constant (C.mol^{-1})
42	R	Ideal gas constant (J.mol^{-1}.K^{-1})

Greek letters

γ_i	Activity coefficient of species i (-)
δ_{ij}	Kronecker delta between species i and j
$\delta_{L,1}$	Film thickness regarding the absorbed gas (m)
μ_i	Chemical potential of species i ($J.mol^{-1}$)
ν_{ij}	Stochiometric coefficient of species i in reaction j (-)
ψ	Local electric potential (V)
ξ_j	Extent of reaction j (-)

Subscripts and superscripts

app	Apparent
calc	Calculated
exp	Experimental
REF	Reference state
1	Absorbed gas
¨	Molality-based asymmetric thermodynamic convention (see Supplementary Material section 2)
~c	Molar concentration-based symmetric thermodynamic convention

1. Introduction

Chemical absorption into basic solutions has been in use since the 1930s for CO_2 separation from raw natural gas or from flue gases (Bottoms, 1931). Solvent screening and design are at the heart of the research effort to increase both CO_2 absorption rate and capacity, and to decrease solvent regeneration duty (e.g., aqueous amine blends). Industrial absorption column design with a given solvent requires the identification of the dissolved gas reaction mechanism. To do so, reactions at equilibrium (e.g., acid-base reactions) and finite-rate reactions need to be studied at pressure, temperature and composition conditions encountered in the absorption column.

Kinetic parameters are typically obtained from absorption or desorption flux measurements in laboratory gas-liquid contactors of known mass transfer coefficient and interfacial area. Most kinetic studies deal with absorption experiments into unloaded basic solutions. Only one irreversible reaction is considered (e.g., (Pohorecki & Moniuk, 1988), (Pani, et al., 1997), (Derks, et al., 2006)). Such studies disregard the increase in ionic strength and non-ideality when CO_2 is absorbed, due to bicarbonate, carbonate, and carbamate ion production. However, absorption models based on activities rather than molarities should lead to more relevant process simulation.

CO_2 absorption modelling into aqueous amine solutions first requires the study of CO_2 reaction with HO^- ion. Indeed, this reaction takes place in all aqueous systems with CO_2. Furthermore, kinetic constants between CO_2 and tertiary amines can be expressed as a function of amine pKa (Couchaux, et al., 2014). Through molecular simulation, (Rozanska, et al., 2021) show that CO_2 kinetics in aqueous tertiary amine solutions can be written as a function of CO_2 and HO^- concentrations only.

For CO_2 absorption into aqueous alkaline salts solutions, researchers choose a one-irreversible-reaction mechanism. In this case, non-ideality is usually included. In early studies such as (Pinsent, et al., 1956), (Hikita, et al., 1976), (Augugliaro & Rizzuti, 1987), (Pohorecki & Moniuk, 1988), and (Kucka, et al., 2002), empirical ionic-strength, alkaline-ion-dependent kinetic constant and CO_2 solubility relations are developed. When studying CO_2 absorption into 30wt% K_2CO_3 solutions, (Thee, et al., 2012) fit one Arrhenius-type expression to their kinetic data between 313 and 353 K. The expression is found coherent with (Knuutila, et al., 2010) correlation when considering identical salt and concentration range. Under relatively diluted Na_2CO_3 and K_2CO_3 concentrations (300 mol/m^3), (Penders-van Elk, et al., 2016) find good agreement of their CO_2 absorption data between 283 and 313 K with pKa-dependent Bronsted kinetic law for tertiary amines. Following (Kucka, et al., 2002), (Haubrock, et al., 2005), (Haubrock, et al., 2007), (Knuutila, et al., 2010) and (Gondal, et al., 2016) develop an activity-based kinetic rate expression, using Pitzer-Debye-Hückel model, empirical activity coefficients and e-NRTL model, respectively. Thus, a unique Arrhenius-type expression applies to all systems (with Li^+, Na^+ or K^+).

(Sheng, et al., 2019) apply current knowledge on CO_2 absorption into aqueous NaOH solutions to measure pilot effective mass transfer area. The influence of five literature sources is evaluated for kinetic and physical properties estimation. According to this study, different Arrhenius parameters result in large variations for the effective mass transfer area estimation. Additionally, inconsistencies between kinetics and physical parameter sources should be avoided.

Absorption involves reversible finite-rate reactions and acid-base reactions at equilibrium. Species simultaneously diffuse to and from gas-liquid interface and react. The diffusion driving force is the

molar concentration gradient in the widely used semi-empirical Fick diffusion law (e.g., (Versteeg, et al., 1989), (Bishnoi & Rochelle, 2002), (Derks, et al., 2006)). However, Maxwell-Stefan theory (Ahmadi, et al., 2010), or Nernst-Planck equation in case of unknown binary diffusivities (e.g., (Glasscock & Rochelle, 1989) and (Littel, et al., 1991)) are more suitable to highly non ideal multiconstituent electrolytic systems. The diffusion driving force is then the chemical potential gradient (Taylor & Krishna, 1993). (Thomas, et al., 2016) model CO_2 diffusion-reaction into stagnant water and aqueous alkaline salt solutions with one irreversible reaction. Instead of individual ion diffusion, salt diffusion across the liquid medium is represented. Thus, diffusivities are decoupled without the need for an electric potential gradient to keep electroneutrality.

Mass transfer problem formulation with any transient or steady-state mass transfer theory results in a set of local balances of each species. The differential problem is a boundary value problem. At the gas-liquid interface, absorbed gas physical equilibrium is assumed and in the liquid bulk, chemical equilibrium is assumed. In some models, acid-base reactions are represented as reversible reactions with a very high reaction rate constant (e.g., (Glasscock & Rochelle, 1989), (Versteeg, et al., 1989), (Ahmadi, et al., 2010)). The problem then includes a system of n_C second order ordinary or partial differential equations. In other models, diffusion-reaction flux coupling is explicitly considered. The number of differential equations decreases, but this formulation lacks generality (e.g., (Rinker, et al., 1995), (Bishnoi & Rochelle, 2002), (Servia, et al., 2014)). This second formulation ensures the n_{eq} acid-base equilibria by the addition of n_{eq} algebraic equations: a differential-algebraic problem needs to be solved.

The purpose of this article is to propose a general reactive absorption model entirely based on activities, unlike previous reactive absorption models. Indeed, previous models are either based on Nernst-Planck diffusion with a complete mass transfer model, but activity coefficients are assumed equal to unity or, like (Gondal, et al., 2016), use a simplified mass transfer model with Fick's diffusion law and constant activity coefficients. Activity coefficients are then calculated at equilibrium with a thermodynamic model. For steady-state absorption, extent-of-reaction variables are introduced to take advantage of flux coupling (section 2). This has two advantages compared to usual model formulations: (1) the number of equations is reduced while still maintaining a general formulation, and (2) solving a system of algebraic equations and substituting the results into the differential equations takes care of acid-base equilibria. Extents of reactions have yet to be implemented in reactive absorption problems.

This model is then applied to CO_2 absorption in aqueous alkaline salts solutions with a full reaction mechanism considering two reversible reactions. This third section aims at fitting a unique Arrhenius-type expression for the direct kinetic constant of reaction $CO_2 + HO^- \leftrightarrow HCO_3^-$ to literature CO_2 absorption flux data with all three alkaline salt counter ions. This part I paves the way to the further study of CO_2 absorption into aqueous amine solutions. Indeed, this reaction takes place in all aqueous solvents. It is necessary to characterise it before focusing on more complex systems.

2. Modelling framework

2.1. Activity-based diffusion, fluxes, rates of reaction and equilibria

Equation 1 gives the Nernst-Planck expression for the diffusion flux of a given species i (Taylor & Krishna, 1993).

$$j_i = -\frac{D_i c_i}{RT}(\nabla \mu_i + z_i \mathcal{F} \nabla \psi) \quad \text{Eq. (1)}$$

In case of different diffusion coefficients of ionic species, the electric potential ψ is to ensure local electroneutrality through the liquid film ($\sum_{i \text{ species}} z_i j_i = 0$):

$$\nabla \psi = -\frac{\sum_{i \text{ species}} z_i D_i c_i \nabla \mu_i}{\mathcal{F} \sum_{i \text{ species}} z_i^2 D_i c_i} \quad \text{Eq. (2)}$$

The chemical potential of a given species i, μ_i, is defined as its partial molar Gibbs free energy (Prausnitz, et al., 1998). A thermodynamic convention consists in defining a reference state, then the activity a_i (eq. 3) and the activity coefficient (eq. SM16 in Supplementary Material) of the species i.

$$\mu_i(T, P, \mathbf{n}) = \left(\frac{\partial G}{\partial n_i}\right)_{T,P,n_{j \neq i}} = \mu_i^{REF}(T, P) + RT \ln(a_i) \quad \text{Eq. (3)}$$

μ_i^{REF} and a_i are expressed in the same chosen thermodynamic convention. The dimension of the activity depends on the composition scale, such as molalities, molarities, mass fractions, etc. We express reaction rates as functions of activities as well (eq. 4).

$$r_j = k_j \left(\prod_{i \text{ species}} a_i^{o_{ij}^D} - \frac{1}{K_j} \prod_{i \text{ species}} a_i^{o_{ij}^R} \right) \quad \text{Eq. (4)}$$

Kinetic constants k_j and equilibrium constants K_j also need to be expressed according to the chosen thermodynamic convention. For reactions assumed to be at equilibrium:

$$K_j = \prod_{i \text{ species}} a_i^{\nu_{ij}} \quad \text{Eq. (5)}$$

ν_{ij} is the stoichiometric coefficient of species i in reaction j. Consistency between orders of reaction and stoichiometric coefficients (eq. 4 and 5) yields $o_{ij}^R - o_{ij}^D = \nu_{ij}$.

Absorption problems are typically one dimension. At gas-liquid interface, the partial pressure and the activity of the absorbed gas (subscript 1) are assumed at equilibrium. A Henry's relation is obtained (Prausnitz, et al., 1998), assuming asymmetric thermodynamic convention for the absorbed gas (eq. 6).

$$H_1 = \frac{p_{1,0}}{a_{1,0}} \quad \text{Eq. (6)}$$

2.2. Extents of reaction and resulting system of equations

For a steady-state mass transfer model such as the film model, a new algebraic variable is introduced: the extent of each reaction. The extent ξ_j of a given reaction j measures its progress in the liquid film from the interface to a distance z. The relation between fluxes and extents of reaction is dictated by stochiometric constraints. The flux of a given species i through the film, as a function of the extents of reaction, is given in eq. 7.

$$j_i = j_{1T,0}\left(\delta_{1i} + \sum_{j \text{ reactions}} \nu_{ij}\xi_j\right) \quad \text{Eq. (7)}$$

Where $j_{1T,0}$ is the total flux of gas absorbed. Due to the normalisation by $j_{1T,0}$, ξ_j is dimensionless. This expression sums up the contribution of extents both finite-rate reactions and reactions assumed at equilibrium where species i is either a reactant or a product. At the gas-liquid interface (z=0), only reactions at equilibrium may have a non-zero extent. For non-volatile species, the extents of all finite-rate reactions must be zero. Eq. 7 then becomes eq. 8 at the gas-liquid interface.

$$j_i(z=0) = j_{1T,0}\left(\delta_{1i} + \sum_{k \text{ reactions}} \nu_{ik}\xi_k(z=0)\right) \quad \text{Eq. (8)}$$

Where index k refers to a reaction assumed at equilibrium. As a result, the flux j_1(z=0) is not only the flux of 1 crossing the interface, $j_{1T,0}$. It is modified by all reactions at equilibrium with a non-zero extent of reaction at the gas-liquid interface (eq. 9).

$$j_1(z=0) = j_{1T,0}\left(1 + \sum_{k \text{ reactions}} \nu_{1k}\xi_k(z=0)\right) \quad \text{Eq. (9)}$$

The local variation of the extent of a finite-rate reaction, is by definition proportional to its local rate (eq. 10).

$$\nabla\xi_j = \frac{r_j}{j_{1T,0}} \quad \text{Eq. (10)}$$

Combining equations 3 and 7 yields eq. 11.

$$j_i = j_{1T,0}\left(\delta_{1i} + \sum_{j \text{ reactions}} \nu_{ij}\xi_j\right) = -\frac{D_i c_i}{RT}(\nabla\mu_i + z_i\mathcal{F}\nabla\psi) \quad \text{Eq. (11)}$$

Differentiation of equilibrium relation (eq. 5) of reaction k generates an algebraic relation between its extent of reaction and the extents of other reactions. Substituting the expression of $\nabla\mu_i$ from eq. 11:

$$0 = \sum_{i \text{ species}} \nu_{ik}\left(j_{1T,0}\frac{\left(\delta_{1i} + \sum_{j \text{ reactions}} \nu_{ij}\xi_j\right)}{D_i c_i} - z_i\mathcal{F}\nabla\psi\right) \quad \text{Eq. (12)}$$

Where index k refers to a given reaction at equilibrium. The resulting system of $n_{R,eq}$ algebraic equations can be solved separately. The resulting extents ξ_k of reactions at equilibrium are substituted back into the differential equations.

2.3. Thermodynamic framework and mass transfer and diffusion assumptions

The mass transfer framework used in this work is the stagnant film theory (Whitman, 1923). In aqueous solution, the asymmetric convention is more relevant for solute species. The selected thermodynamic model is described in the Supplementary Material section 2. Ionic diffusivities are known only in water at infinite dilution at 25°C. As a first application, equal diffusivities are assumed

for all ions in solution (as did e.g., (Derks, et al., 2006), (Ahmadi, et al., 2010), (Luo, et al., 2015)). The electric potential term is thus neglected. Since the problem is spatially one-dimensional (in z), eq. 13 is obtained.

$$j_i = -D_i \sum_{k \text{ species}} \left(\delta_{ik} + c_i \frac{\partial \ln \ddot{\gamma}_i}{\partial c_k} \right) \frac{dc_k}{dz} \qquad \text{Eq. (13)}$$

Where $\ddot{\gamma}_i$ is the activity coefficient of species i in the molality-based asymmetric convention, and δ_{ik} is the Kronecker delta (1 if i=k, 0 otherwise). Reactions rates can be expressed as:

$$r_j = \tilde{k}_j^c \left(\prod_{i \text{ species}} (\tilde{\gamma}_i c_i)^{o_{ij}^D} - \frac{1}{\tilde{K}_j^c} \prod_{i \text{ species}} (\tilde{\gamma}_i c_i)^{o_{ij}^R} \right) \qquad \text{Eq. (14)}$$

Where $\tilde{\gamma}_i = \frac{\ddot{\gamma}_i}{x_{\mathrm{H_2O}}}$ is the activity coefficient of species i in the molarity-based asymmetric convention. $\tilde{k}_j^c(T)$ is the forward kinetic constant of reaction j ($\left(\mathrm{m^3.mol^{-1}}\right)^{\sum o_{ij}^D}.\mathrm{s^{-1}}$) and $\tilde{K}_j^c(T)$ is the equilibrium constant of reaction j ($\left(\mathrm{m^3.mol^{-1}}\right)^{\sum \nu_{ij}}$). Both are written in the same convention.

Reaction equilibrium equations are then written as follows.

$$\tilde{K}_j^c = \prod_{i \text{ species}} (\tilde{\gamma}_i c_i)^{\nu_{ij}} \qquad \text{Eq. (15)}$$

Combining equations 3 and 14 yields eq. 16.

$$j_i = j_{1T,0} \left(\delta_{1i} + \sum_{j \text{ reactions}} \nu_{ij} \xi_j \right) = -D_i \sum_{k \text{ species}} \left(\delta_{ik} + c_i \frac{\partial \ln \ddot{\gamma}_i}{\partial c_k} \right) \frac{dc_k}{dz} \qquad \text{Eq. (16)}$$

Without electric potential gradient, the system of equations defined by eq. 12 becomes linear regarding the extents of reactions at equilibrium:

$$0 = \frac{\nu_{1k}}{c_1 D_1} + \sum_{i \text{ species}} \frac{\nu_{ik}}{c_i D_i} \sum_{j \text{ reactions}} \nu_{ij} \xi_j \qquad \text{Eq. (17)}$$

In the chosen thermodynamic convention, Henry's relation for the absorbed gas at the interface (z=0) is expressed as follows:

$$p_{1,0} = \frac{H_1(T, P, \mathbf{n})}{c_{\mathrm{H_2O}}} \ddot{\gamma}_1 c_{1,0} \qquad \text{Eq. (18)}$$

As experimental pressure is lower than 1 bar in the data considered in section 3, gas-phase is assumed ideal.

2.4. Solution

Before writing the differential problem to solve, dimensionless variables (eq. 19) and parameters (eq. 20) are introduced.

$$Z = \frac{z}{\delta_{L,1}} = \frac{k_{L,1}}{D_1} z$$

$$C_i = \frac{c_i}{c_{N,i}} \qquad \text{Eq. (19)}$$

Where $c_{N,i}$ is the normalising concentration, such as if i=1, $c_{N,i} = c_{1,0}$, and $c_{N,i} = c_{abs,tot}$ otherwise. $c_{abs,tot}$ is the total absorptive species concentration (mol.m^{-3}).

$$Z_{D,i} = \frac{c_{N,i} D_i}{c_{1,0} D_1}$$

$$E = \frac{j_{1T,0}}{k_{L,1} c_{1,0}}$$

$$\mathrm{Ha}_j^2 = \frac{D_1 \tilde{k}_j^c \left(\prod_i \left(c_{N,i} \right)^{o_{ij}^D} \right)}{k_{L,1}^2 c_{1,0}} \qquad \text{Eq. (20)}$$

$$K_{N,j} = \prod_i \left(c_{N,i} \right)^{\nu_{ij}}$$

Therefore, the flux of species i is expressed as a matrix product (eq. 21).

$$j_i = j_{1T,0} \left(\delta_{1i} + \sum_{j \text{ reactions}} \nu_{ij} \xi_j \right) = -j_{1T,0} \frac{Z_{D,i}}{E} \sum_{k \text{ species}} M_{ik} \frac{dC_k}{dZ}$$

$$M_{ik} = \left(\delta_{ik} + C_i \frac{\partial \ln \ddot{\gamma}_i}{\partial C_k} \right) \qquad \text{Eq. (21)}$$

Square matrix M inversion yields:

$$\frac{dC_k}{dZ} = -\mathrm{E} \left(\sum_{i \text{ species}} (M^{-1})_{ki} X_i \right) \qquad k = 1..n_C$$

$$\frac{d\xi_j}{dZ} = \frac{\mathrm{Ha}_j^2}{E} \left(\prod_{i \text{ species}} (\tilde{\gamma}_i C_i)^{o_{ij}^D} - \frac{K_{N,j}}{\tilde{K}_j^c} \prod_{i \text{ species}} (\tilde{\gamma}_i C_i)^{o_{ij}^R} \right) \qquad j = 1..n_{\mathrm{R,kin}} \qquad \text{Eq. (22)}$$

Where M^{-1} is the inverse of matrix M and vector X is defined as $X = \left(\frac{\delta_{1i} + \sum_{j \text{ reactions}} \nu_{ij} \xi_j}{Z_{Di}} \right)_i$.

At each resolution step, an algebraic system of equations is solved independently to obtain the extents of acid-base reactions (eq. 23). These values are used in the differential equations.

$$0 = \frac{\nu_{1k}}{C_1} + \sum_{i \text{ species}} \frac{\nu_{ik}}{Z_{D,i} C_i} \sum_{j \text{ reactions}} \nu_{ij} \xi_j \qquad \text{Eq. (23)}$$

Boundary conditions are presented in Table 1.

Table 1 Film model boundary conditions with dimensionless variables

$Z = 0\ (z = 0)$	$Z = 1\ (z = \delta_{L,1})$
$C_1 = 1$	$C_i = \frac{c_{b,i}}{c_{N,i}}, \forall i$ species in solution
$\xi_j = 0, \forall j$ finite-rate reaction	-

This formulation with Nernst-Planck equation for molecular diffusion and activity-based rate expressions consists in a system of $n_C+n_{R,kin}$ *first*-order ordinary differential equations, thanks to steady-state extents of reaction, whereas writing local balances per species leads to a system of n_C *second*-order differential equations. Extents of reactions at equilibrium are calculated from a set of $n_{R,eq}$ algebraic equations (eq. 23). Equilibrium relations, Nernst-Planck diffusion fluxes and reaction rates are activity-based. Therefore, this model reconciles kinetics and thermodynamics especially close to equilibrium. Simulations are performed in Matlab R2013a. The bvp4c function available in the software is used to solve the differential problem (Kierzenka & Shampine, 2001).

3. Application to alkaline salts-water-CO_2 systems

Four species are considered: CO_2, HCO_3^-, CO_3^{2-} and HO^- (n_C=4). The alkaline ion does not take part in the reaction scheme, so that its concentration is constant through the film because the electric potential is disregarded. However, this ion contributes to non-ideality. The mechanism consists in two reversible reactions (n_R=2):

$$CO_2 + HO^- \leftrightarrow HCO_3^- \quad \text{(R-I)}$$

$$HCO_3^- + HO^- = CO_3^{2-} + H_2O \quad \text{(R-II)}$$

Reaction R-I is reversible and finite-rate ($n_{R,kin}$=1):

$$r_{\mathrm{I}} = r_{(CO_2,HO^-)} = \tilde{k}^c_{(CO_2,HO^-)} \left(\tilde{\gamma}_{CO_2} \tilde{\gamma}_{(HO^-)} c_{CO_2} c_{(HO^-)} - \frac{\tilde{\gamma}_{(HCO_3^-)} c_{(HCO_3^-)}}{\tilde{K}^c_{(CO_2,HO^-)}} \right) \quad \text{Eq. (24)}$$

Where $\tilde{k}^c_{(CO_2,HO^-)}$ is its forward kinetic constant – to determine – ($m^3.mol^{-1}.s^{-1}$) and $\tilde{K}^c_{(CO_2,HO^-)}$ its equilibrium constant ($m^3.mol^{-1}$).

In addition, the acid-base equilibrium between HCO_3^- and CO_3^{2-} is considered (reaction R-II; $n_{R,eq}$=1).

The equilibrium constant parameters are taken from (Kamps, et al., 2001). Solution density is taken from (Laliberté & Cooper, 2004). Liquid phase CO_2 diffusivity is calculated with the Stokes-Einstein relation (Versteeg & Van Swaaij, 1988). (Knuutila, et al., 2010) use this relation as well in combination with CO_2 diffusivity in pure water from (Danckwerts & Lannus, 1970). Viscosity is taken from (Laliberté, 2007). Hydroxide ion diffusivity is set to $1.7\times D_{CO2}$ based on the ratio proposed by (Hikita, et al., 1976), and $D_{(HCO3-)}$ and $D_{(CO32-)}$ are supposed equal to $D_{(HO-)}$ (see Supplementary Material section 1 for detailed correlations).

As a base case, the mass transfer model was tested with no deviation from ideality (γ=1) and (Weisenberger & Schumpe, 1996) CO_2 apparent solubility ("concentration-based model"). Secondly, the activity-based model was implemented.

Few CO_2 absorption flux measurements are available in these systems. (Kucka, et al., 2002), (Pohorecki & Moniuk, 1988) and (Knuutila, et al., 2010) do not publish raw experimental data, such as CO_2 partial pressure. (Gondal, et al., 2016) use raw absorption flux data from (Gondal, et al., 2015) in alkaline hydroxide solutions and from (Knuutila, et al., 2010) in alkaline carbonate solutions. Note that data from (Knuutila, et al., 2010) is not available in open literature. The only other raw dataset on CO_2 absorption in sodium hydroxide and carbonate solutions was found in (Hikita, et al., 1976) (see Table 2).

Table 2 Available CO_2 absorption flux data in alkaline hydroxide and carbonate aqueous solutions

Ref, apparatus	Alk^+	$x(Alk^+,app)$	$x(HO^-,app)$	$x(CO_2,app)$	T (K)	P_{CO2} (kPa)	n_{data}
(Gondal, et al., 2015), SDC	Li^+	$1.8.10^{-4}$-0.035	$1.8.10^{-4}$-0.035	0-$3.5.10^{-4}$	298-338	0.17-0.28	30
(Hikita, et al., 1976), Jet & WWC	Na^+	$2.3.10^{-3}$-0.025	0-$9.0.10^{-3}$	$2.3.10^{-7}$-0.017	298-303	100	157
(Gondal, et al., 2015), SDC	Na^+	$1.8.10^{-4}$-0.036	$1.8.10^{-4}$-0.036	0-$3.6.10^{-4}$	298-333	0.18-0.32	38
(Gondal, et al., 2015), SDC	K^+	$1.6.10^{-4}$-0.033	$1.6.10^{-4}$-0.033	0-$3.6.10^{-4}$	298-337	0.16-0.29	35

SDC: "String of Discs Column", Jet: "Laminar Jet Absorber", WWC: "Wetted-Wall Column", Alk^+: alkaline ion.

For kinetic constant regression, (Gondal, et al., 2015) data was used, as it encompasses all three alkaline ions between 298 and 338 K. To keep datasets with each counter ion approximately to the same size, (Hikita, et al., 1976) data for sodium hydroxide and carbonate solutions between 298 and 303 K was used as a validation dataset. (Hikita, et al., 1976) data therefore also serves as a model prediction test. Modelling each flux measurement requires the value of the liquid-side mass transfer coefficient, which is taken from each study.

Kinetic parameter optimisation of reaction R-I direct kinetic constant is achieved using the objective function specified in eq. 25.

$$f_{\text{obj}} = \sum_{i\ \text{data}} \frac{1}{2}\left(\left(\frac{j_i^{\text{calc}} - j_i^{\text{exp}}}{j_i^{\text{exp}} + \varepsilon}\right)^2 + \left(\frac{j_i^{\text{calc}} - j_i^{\text{exp}}}{j_i^{\text{calc}} + \varepsilon}\right)^2\right) \qquad \text{Eq. (25)}$$

ε is a constant set to 1.10^{-4} $mol.m^{-2}.s^{-1}$ to mitigate the error value for very small absorption fluxes. The two terms in the objective function (eq. 25) give this function a symmetrical behaviour for flux underestimation and overestimation. Optimisation function fminsearch from Matlab R2013a was used to fit the Arrhenius parameters of the kinetic constant (eq. 26). In fminsearch, the simplex algorithm by (Lagarias, et al., 1998) is used.

$$\ln k_{(CO_2,HO^-)} = A + \frac{E_A}{RT} \qquad \text{Eq. (26)}$$

The fitted Arrhenius parameters as well as model performance is presented in Table 3: the average absolute deviation (AAD, eq. 27) and the bias (eq. 28) of regression (Gondal, et al., 2015) and validation (Hikita, et al., 1976) datasets. Model performance is also compared to (Gondal, et al., 2016).

$$\mathrm{AAD} = \frac{1}{n_{\mathrm{data}}} \sum_{i\ \mathrm{data}} \left| \frac{j_i^{\mathrm{calc}} - j_i^{\mathrm{exp}}}{j_i^{\mathrm{exp}}} \right| \times 100 \qquad \text{Eq. (27)}$$

$$\mathrm{bias} = \frac{1}{n_{\mathrm{data}}} \sum_{i\ \mathrm{data}} \frac{j_i^{\mathrm{calc}} - j_i^{\mathrm{exp}}}{j_i^{\mathrm{exp}}} \times 100 \qquad \text{Eq. (28)}$$

Parameter standard errors are calculated by variance-covariance analysis, as described in the Supplementary Material section 3.

Table 3 Optimised Arrhenius parameters of reaction R-I direct kinetic constant over (Gondal, et al., 2015) CO_2 absorption flux data in alkaline hydroxide solutions and performance

Model		Concentration-based	Activity-based	(Gondal, et al., 2016)
	A	19.387 ± 0.004	19.841 ± 0.003	19.53
Reference	E_A/R (K)	-5020.99 ± 0.07	-5248.77 ± 0.05	-5111.2
(Gondal, et al., 2015) (Li^+, Na^+, K^+)	AAD (%)	14	10	15
	Bias (%)	6.2	-2.1	-
(Hikita, et al., 1976) (Na^+)	AAD (%)	17	14	-
	Bias (%)	12	-0.23	-

Remark: (Gondal, et al., 2016) do not provide parameter standard deviations.

Parity and deviation plots are shown in Figure 1 and Figure 2, respectively.

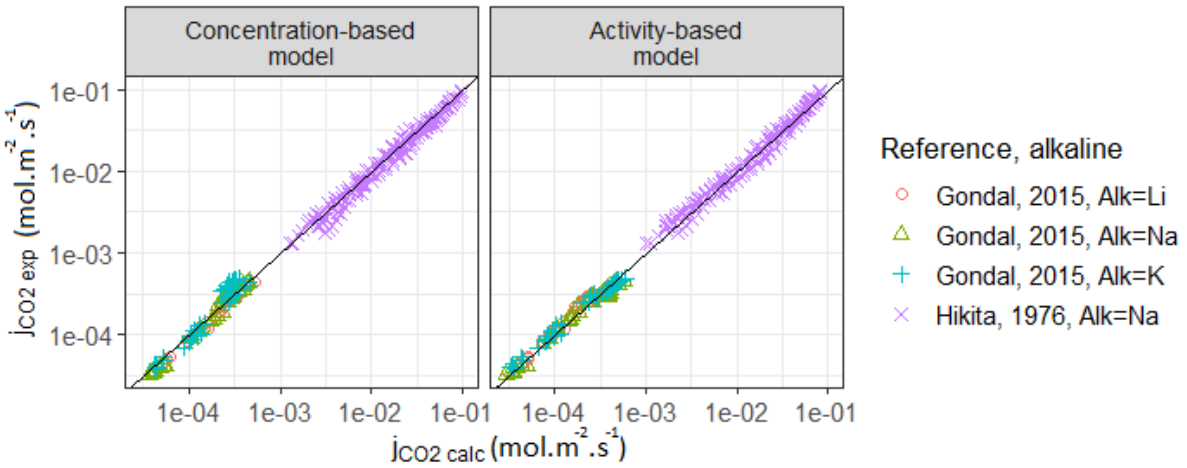

Figure 1 Reactive absorption model parity plot for alkaline salts-water-CO_2 systems

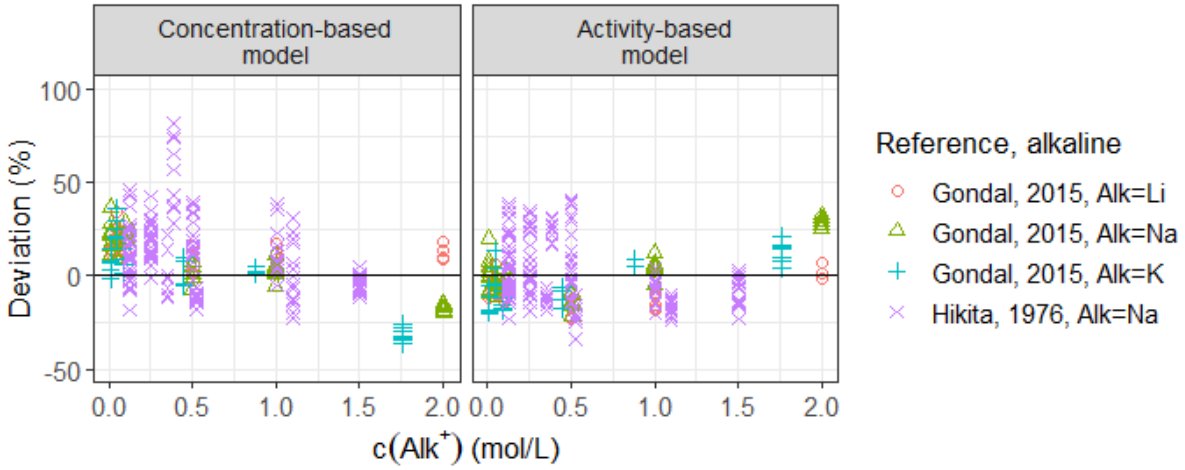

277

278 **Figure 2** Reactive absorption model deviations for alkaline salts-water-CO_2 systems

279 Considering solution non-ideality improves model performance for all three types of salts. The only
280 exception is the data of (Gondal, et al., 2015) with NaOH data at 2 $mol.L^{-1}$. All data from (Gondal, et
281 al., 2015) for all three salts (Li, Na and K-based) and most of the data from (Hikita, et al., 1976) are
282 represented within a +/-30% relative deviation by the activity-based model. Only 13 of all 157
283 validation data points have a relative deviation exceeding +/-30%. AAD over validation dataset is
284 13,7% and bias -0,2%, which is on par with the model performance of (Gondal et al., 2016).
285 Concentration-based model performance is on par with that of (Gondal, et al., 2016) when
286 considering the data of (Gondal, et al., 2015). Ideal solution is assumed in the concentration-based
287 model for reaction rate, diffusion flux, and chemical equilibria, but uses a correlation for CO_2 physical
288 solubility at gas-liquid interface. Salting-out effect on CO_2 solubility due to increasing ionic strength is
289 represented in both models: in the concentration-based model, by ion-concentration-dependent
290 (Weisenberger & Schumpe, 1996) correlation, and in the activity-based model, by the developed
291 thermodynamic model (see Supplementary Material section 2). Finally, only the activity-based model
292 unifies the representation of all equilibria with the chosen thermodynamic model, whereas the
293 concentration-based model is correlation-dependent.

294 The activity-based model is better at predicting (Hikita, et al., 1976) measurements in NaOH and
295 Na_2CO_3 aqueous solutions than the concentration-based model. This suggests the activity-based
296 model can more easily be extrapolated outside regression area than the concentration-based model.

297 Arrhenius parameters are compared to previous studies in Figure 3, specifically (Pohorecki & Moniuk,
298 1988), (Kucka, et al., 2002), (Knuutila, et al., 2010) and (Gondal, et al., 2016). All these studies
299 consider the solution non ideality in the reaction rate expression. Both concentration-based and
300 activity-based models lead to close kinetic constants compared to (Gondal, et al., 2016). The
301 Arrhenius law obtained with the activity-based model displays a -14% to -9% difference in the
302 regression temperature range.

303 Fitted Arrhenius law extrapolation to higher temperatures leads to significant underestimation
304 compared to the kinetic constant obtained by (Knuutila, et al., 2010) with their own experimental
305 data and methodology – 94 vs. 157 $m^3.mol^{-1}.s^{-1}$ at 343 K. The value remains close to that of (Gondal,
306 et al., 2016) – 102 $m^3.mol^{-1}.s^{-1}$. Temperatures of 343 K and higher occur in industrial absorption

columns. Therefore, having access to raw absorption flux data at higher temperatures (e.g., found in (Knuutila, et al., 2010)) is of interest to extend kinetic law application range.

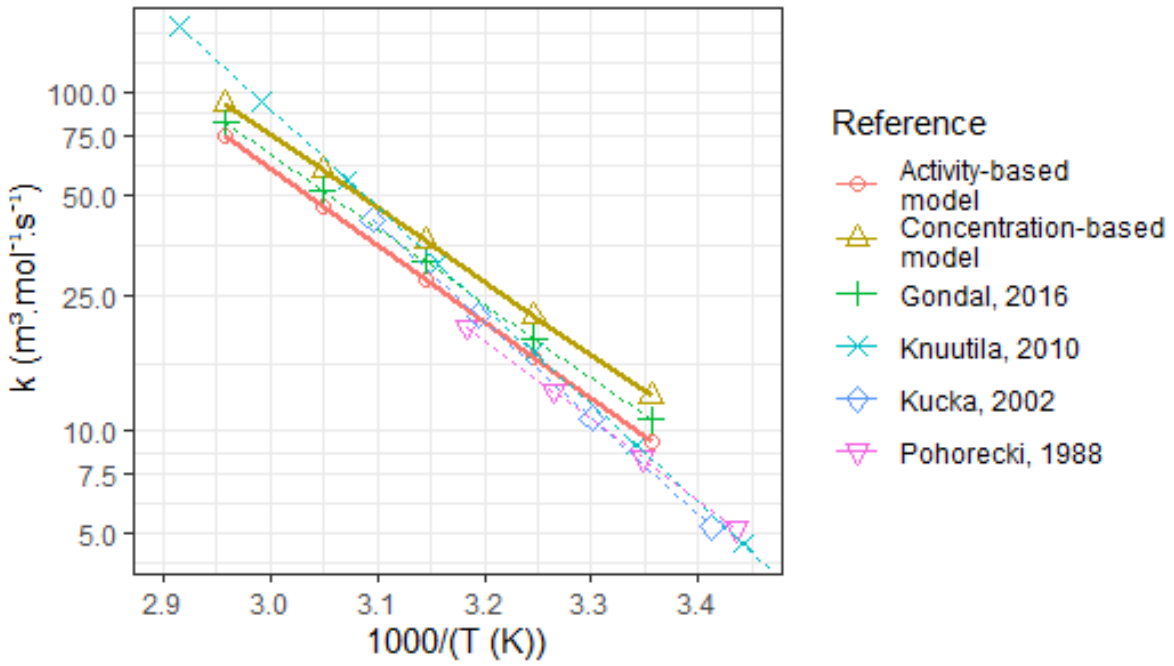

Figure 3 Arrhenius plot and comparison to previous studies

Activity-based model results at specific conditions are then examined. Theses conditions are listed in in Table 4. The four selected points cover the examined data experimental conditions (type and concentration of salt, temperature, CO_2 partial pressure). As a reminder, CO_2 concentration is normalised by $c_{1,0}$, its concentration at the interface, while all other concentrations are normalised by $c_{abs,tot} = c_{(Alk+)}$.

Table 4 Selected points for concentration, extent of reaction and activity coefficient profile simulation: system and conditions

Figure	Reference	Salt	c_{salt} (mol.L^{-1})	T (K)	P_{CO2} (kPa)	$k_{L,1}$ (m.s^{-1})	$c_{1,0}$ (mol.L^{-1})*
Figure 4	(Gondal, et al., 2015)	LiOH	0.01	336	0.2	$1.7.10^{-4}$	$3.1.10^{-5}$
Figure 5	(Gondal, et al., 2015)	KOH	1.76	317	0.2	$1.1.10^{-4}$	$2.6.10^{-5}$
Figure 6	(Hikita, et al., 1976)	Na_2CO_3	0.06	298	100	$5.0.10^{-5}$	$32.0.10^{-3}$
Figure 7	(Hikita, et al., 1976)	NaOH	0.13	303	100	$4.5.10^{-5}$	$28.2.10^{-3}$

*Calculated variable (eq. 18), in the activity-based model

Concentration and extent of reaction profiles calculated with non-ideality consideration (solid lines and symbols in Figure 4 to Figure 7) or with ideal solution hypothesis (dashed lines in Figure 4 to Figure 7) display similar trends. CO_2 concentration profiles are especially close in both models. Consequently, resulting Arrhenius parameters are very close in both models as well. As expected, in these systems and at these conditions, calculated activity coefficient profiles are mostly constant but largely different from unity. Other more complex systems, such as acid gas absorption into aqueous amine solutions, could lead to higher non-ideality influence.

(Gondal, et al., 2015) experiments are compatible with pseudo-first order absorption regime assumption (Figure 4 and Figure 5). Concentration profiles are compatible with this assumption: HO^- concentration barely drops at the interface. The main reaction product is not HCO_3^-, but CO_3^{2-}, and extents of both reactions are close along the liquid film. They are even the equal in Figure 5. This is because CO_3^{2-} (pKb(25°C) = 3,7) is more basic than HCO_3^- (pKb(25°C) = 7,3). At these conditions, activity coefficients are constant, as the overall solution composition remains close to bulk composition everywhere. Still, activity coefficients differ significantly from unity and non ideality needs to be considered. Therefore, according to the model, (Gondal, et al., 2015) absorption flux measurements can be interpreted with constant activity coefficients (as done by (Gondal, et al., 2015) and (Gondal, et al., 2016)). The same behaviour, but amplified, is displayed in Figure 5. HO^- excess is much more important, therefore, reaction R-II equilibrium shifts toward CO_3^{2-} formation. Activity coefficient divergence from unity is significantly higher, due to very high ionic strength.

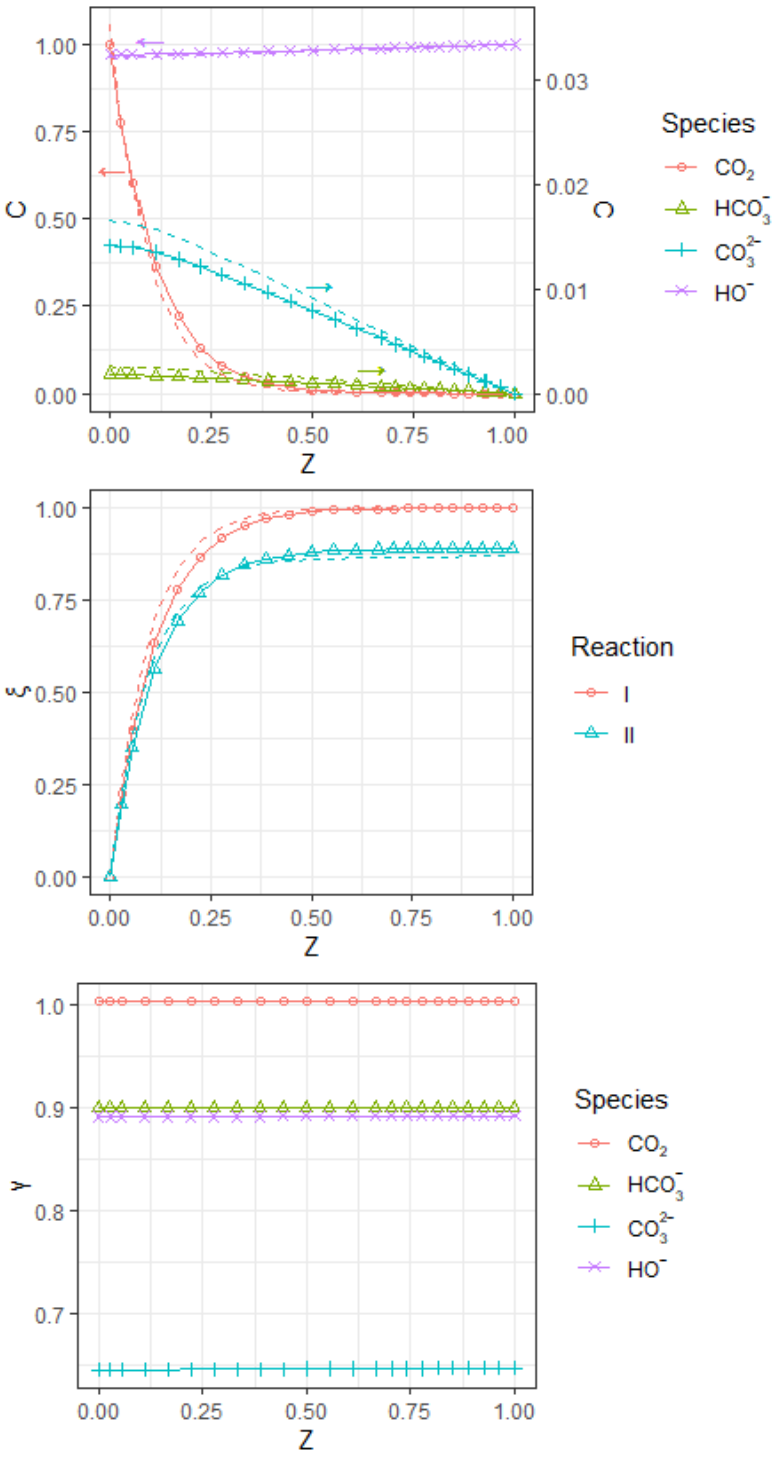

338

339 **Figure 4** Simulated absorption of CO_2 in LiOH aqueous solution at 0.01 mol.L^{-1}, 336 K and P_{CO2} = 0.2
340 kPa measured by (Gondal, et al., 2015). C: normalised concentration, ξ: extent of reaction, γ: activity
341 coefficient. Solid line & symbol: activity-based model, dashed line: concentration-based model (C and
342 ξ). γ_{Li+} = 0.88

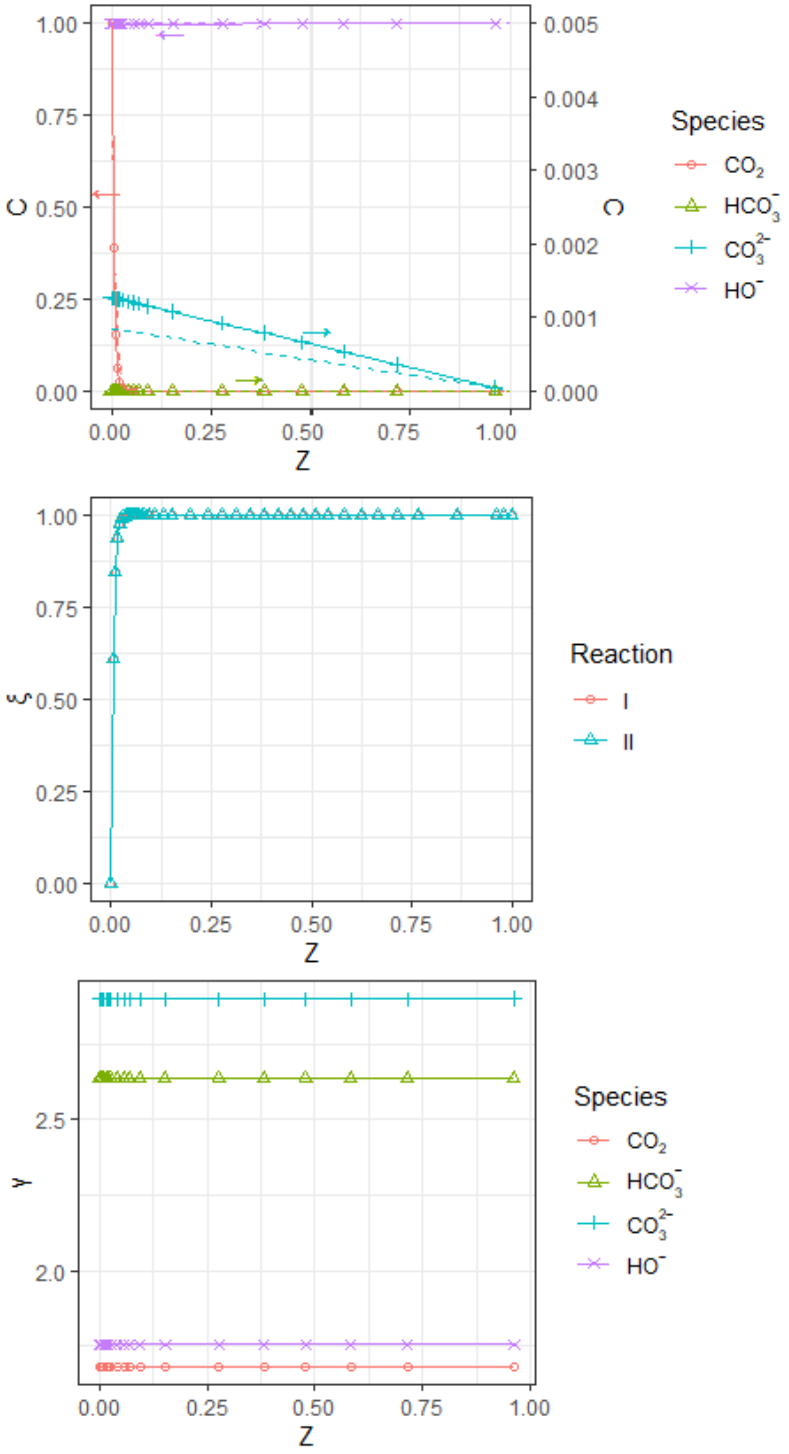

Figure 5 Simulated absorption of CO_2 in KOH aqueous solution at 1.76 mol.L^{-1}, 317 K and P_{CO2} = 0.2 kPa measured by (Gondal, et al., 2015). C: normalised concentration, ξ: extent of reaction, γ: activity coefficient. Solid line & symbol: activity-based model, dashed line: concentration-based model (C and ξ). γ_{K+} = 1.48

In Figure 6, resulting CO_2 absorption profiles are shown in aqueous Na_2CO_3 at conditions researched by (Hikita, et al., 1976). In this case, the main reaction product is HCO_3^- from CO_3^{2-} conversion. This is also coherent with a negative extent of reaction R-II. Here, reversibility needs to be considered,

which the model does, unlike models from the literature (e.g., (Knuutila, et al., 2010), (Gondal, et al., 2016)).

Activity coefficients display a gradient along the liquid film in Figure 7, with a maximum of 14% decrease from liquid bulk to interface for $\gamma_{(CO32-)}$. In (Hikita, et al., 1976), experimental CO_2 partial pressure is of several orders of magnitude higher than in (Gondal, et al., 2015) – 100 vs. 0.2 kPa. HO^- concentration drops significantly along the liquid film, more so close to the interface, in a similar behaviour to the instantaneous absorption regime. CO_3^{2-} is consumed in the vicinity of the interface. At these experimental conditions, it is important to consider the reaction mechanism with both reactions and varying activity coefficients along the liquid film. The high absorption driving force results in ionic strength variation. These conditions are closer to those expected in an industrial setting. This shows how the model could accurately represent mass transfer phenomena at industrial conditions.

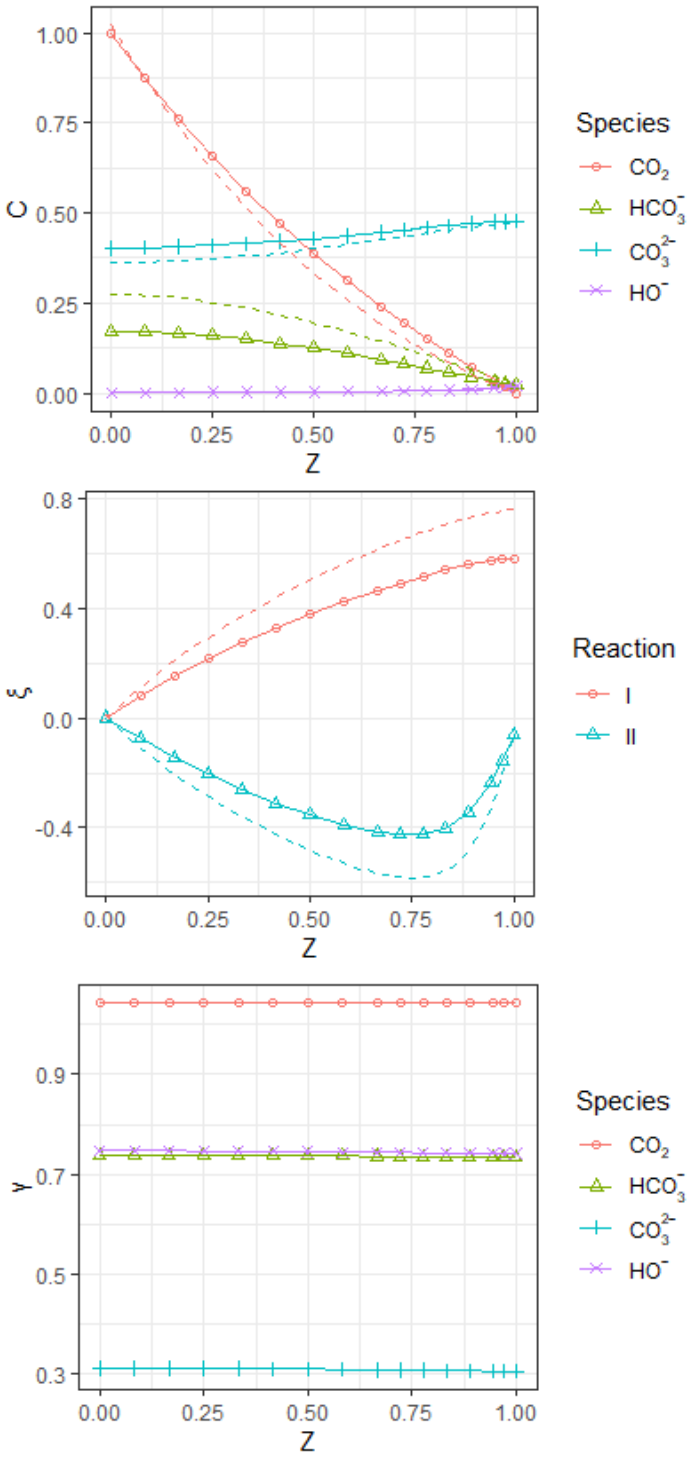

363

364 **Figure 6** Simulated absorption of CO_2 in Na_2CO_3 aqueous solution at 0.06 mol.L^{-1}, 298 K and P_{CO2} =
365 100 kPa measured by (Hikita, et al., 1976). C: normalised concentration, ξ: extent of reaction, γ:
366 activity coefficient. Solid line & symbol: activity-based model, dashed line: concentration-based
367 model (C and ξ). γ_{Na+} = 0.68

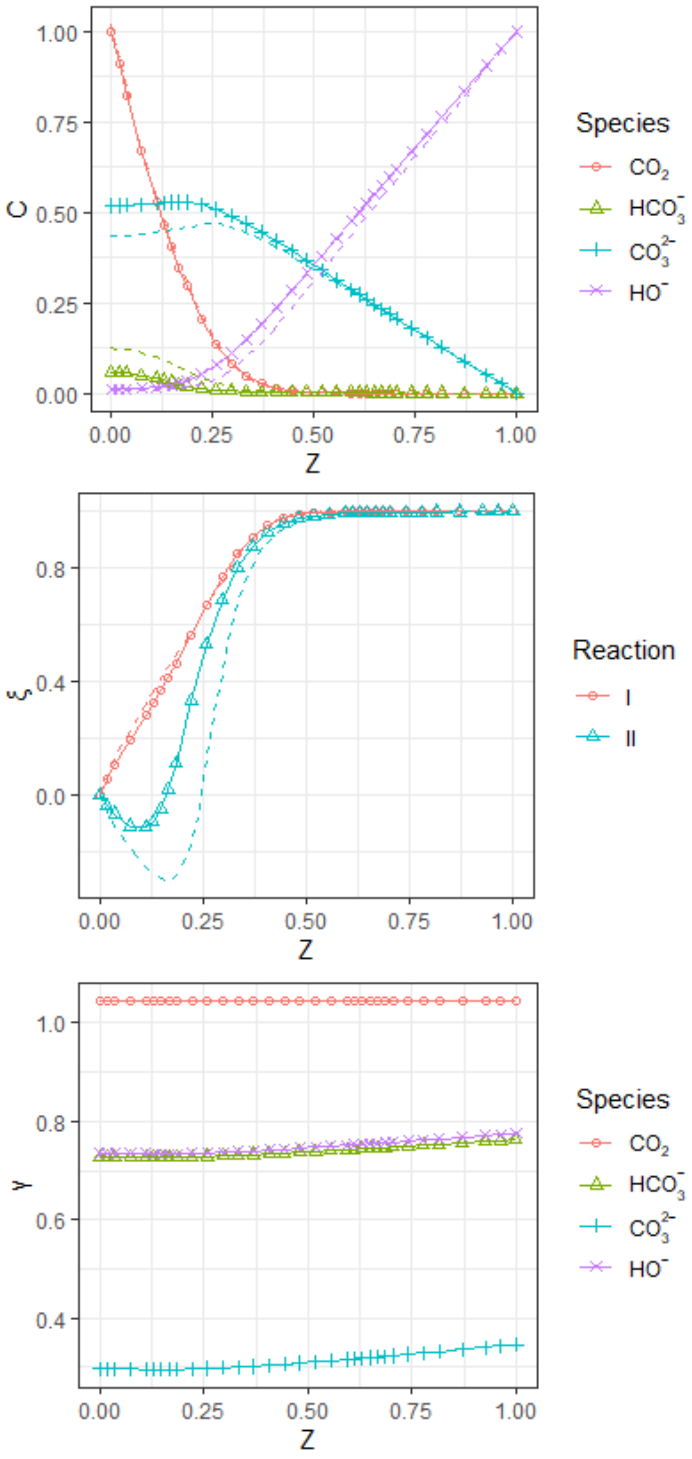

Figure 7 Simulated absorption of CO_2 in NaOH aqueous solution at 0.13 mol.L^{-1}, 303 K and P_{CO2} = 100 kPa measured by (Hikita, et al., 1976). C: normalised concentration, ξ: extent of reaction, γ: activity coefficient. Solid line & symbol: activity-based model, dashed line: concentration-based model (C and ξ). γ_{Na+} = 0.76

4. Conclusion

This study implements a steady-state reactive absorption model applied to the stagnant film theory and focusing on solution non-ideality representation in equilibrium relations, Nernst-Planck diffusion fluxes and reaction rates. This approach is more complete than literature models where activity

coefficients are assumed constant, and most often equal to unity. Extents of reactions, a new feature for reactive absorption models, reduces the number of differential problem variables while maintaining a general formulation. This formulation with Nernst-Planck equation for molecular diffusion and activity-based rate expressions consists in a system of $n_C+n_{R,kin}$ *first*-order ordinary differential equations, whereas writing local balances per species leads to a system of n_C *second*-order differential equations. The relation between fluxes and extents of reactions is dictated by stochiometric constraints.

This model is first applied to alkaline salts-water-CO_2 systems and the CO_2 absorption flux data from the literature. Arrhenius parameters for $CO_2 + HO^- \leftrightarrow HCO_3^-$ direct kinetic constant are fitted. This is a necessary step to study amine-based systems in the same modelling framework. This progressive approach is made possible by the kinetic data availability in alkaline salts-water-CO_2 systems. The obtained Arrhenius parameters are coherent to previous studies in the regression temperature interval. Overall AAD is 12%. Besides, the consideration of activity coefficient variation along the liquid film is shown to be relevant when experimental conditions diverge from the simple pseudo-first order absorption regime. These conditions are closer to the industrial setting.

Model improvement perspectives include extending mass transfer representation to steady-state eddy-diffusivity theory, and assessing uncoupled ion diffusivities influence.

With this model, reaction mechanism investigation in any reactive absorption system is possible. Our further goal is to apply the model to CO_2 absorption in aqueous amines solutions (namely MDEA), especially for increasing CO_2 partial pressure and loading. In these solutions, the more complex reaction scheme could lead to higher variations in ionic strength and activity coefficients through the liquid film.

Acknowledgements

Pr. Alain Gaunand and Pr. Christophe Coquelet would like to acknowledge TotalEnergies for their research partnership and financial support, and the authors would like to acknowledge the Agence Nationale de la Recherche et de la Technologie (ANRT) for their financial support (Cifre 2018/1069).

References

Ahmadi, A. et al., 2010. Rigorous Multicomponent Reactive Separations Modelling: Complete Consideration of Reaction-Diffusion Phenomena. *Oil & Gas Science and Technology-Revue d'IFP Energies nouvelles,* 65(5), pp. 735-749.

Augugliaro, V. & Rizzuti, L., 1987. Kinetics of carbon dioxide absorption into catalysed potassium carbonate solutions. *Chemical Engineering Science,* 42(10), pp. 2339-2343.

Bishnoi, S. & Rochelle, G. T., 2002. Absorption of carbon dioxide in aqueous piperazine/methyldiethanolamine. *AIChE Journal,* 48(12), pp. 2788-2799.

Bottoms, R. R., 1931. Organic bases for gas purification. *Industrial & Engineering Chemistry,* 23(5), pp. 501-504.

Couchaux, G. et al., 2014. Kinetics of carbon dioxide with amines. I. Stopped-flow studies in aqueous solutions. A review. *Oil & Gas Science and Technology - Revue d'IFP Energies nouvelles,* 69(5), pp. 865-884.

Danckwerts, P. V. & Lannus, A., 1970. Gas-Liquid Reactions. *Journal of The Electrochemical Society,* 117(10), p. 369.

Derks, P. W. et al., 2006. Kinetics of absorption of carbon dioxide in aqueous piperazine solutions. *Chemical Engineering Science,* 61(20), pp. 6837-6854.

Glasscock, D. A. & Rochelle, G. T., 1989. Numerical simulation of theories for gas absorption with chemical reaction. *AIChE Journal,* 35(8), pp. 1271-1281.

Gondal, S., Asif, N., Svendsen, H. F. & Knuutila, H., 2015. Kinetics of the absorption of carbon dioxide into aqueous hydroxides of lithium, sodium and potassium and blends of hydroxides and carbonates. *Chemical Engineering Science,* Volume 123, pp. 487-499.

Gondal, S., Svendsen, H. F. & Knuutila, H. K., 2016. Activity based kinetics of CO2--OH- systems with Li+, Na+ and K+ counter ions. *Chemical Engineering Science,* Volume 151, pp. 1-6.

Haubrock, J., Hogendoorn, J. A. & Versteeg, G. F., 2005. The applicability of activities in kinetic expressions: a more fundamental approach to represent the kinetics of the system CO2-OH-in terms of activities. *International Journal of Chemical Reactor Engineering,* 3(1).

Haubrock, J., Hogendoorn, J. A. & Versteeg, G. F., 2007. The applicability of activities in kinetic expressions: A more fundamental approach to represent the kinetics of the system CO2-OH--salt in terms of activities. *Chemical Engineering Science,* 62(21), pp. 5753-5769.

Hikita, H., Asai, S. & Takatsuka, T., 1976. Absorption of carbon dioxide into aqueous sodium hydroxide and sodium carbonate-bicarbonate solutions. *The Chemical Engineering Journal,* 11(2), pp. 131-141.

Kamps, A. P.-S. et al., 2001. Solubility of single gases carbon dioxide and hydrogen sulfide in aqueous solutions of N-methyldiethanolamine at temperatures from 313 to 393 K and pressures up to 7.6 MPa: New experimental data and model extension. *Industrial & engineering chemistry research,* 40(2).

Kierzenka, J. & Shampine, L. F., 2001. A BVP solver based on residual control and the Maltab PSE. *ACM Transactions on Mathematical Software (TOMS),* 27(3), pp. 299-316.

Knuutila, H., Juliussen, O. & Svendsen, H. F., 2010. Kinetics of the reaction of carbon dioxide with aqueous sodium and potassium carbonate solutions. *Chemical Engineering Science,* 65(23), pp. 6077-6088.

Kucka, L., Kenig, E. Y. & Gorak, A., 2002. Kinetics of the gas- liquid reaction between carbon dioxide and hydroxide ions. *Industrial & Engineering Chemistry Research,* 41(24), pp. 5952-5957.

Lagarias, J. C., Reeds, J. A., Wright, M. H. & Wright, P. E., 1998. Convergence properties of the Nelder--Mead simplex method in low dimensions. *SIAM Journal on optimization,* 9(1), pp. 112-147.

Laliberté, M., 2007. Model for calculating the viscosity of aqueous solutions. *Journal of Chemical & Engineering Data,* 52(2), pp. 321-335.

Laliberté, M. & Cooper, W. E., 2004. Model for calculating the density of aqueous electrolyte solutions. *Journal of Chemical & Engineering Data,* 49(5), pp. 1141-1151.

Littel, R. J., Filmer, B., Versteeg, G. F. & Van Swaaij, W. P., 1991. Modelling of simultaneous absorption of H2S and CO2 in alkanolamine solutions: the influence of parallel and consecutive reversible reactions and the coupled diffusion of ionic species. *Chemical Engineering Science,* 46(9), pp. 2303-2313.

Luo, X., Hartono, A., Hussain, S. & Svendsen, H. F., 2015. Mass transfer and kinetics of carbon dioxide absorption into loaded aqueous monoethanolamine solutions. *Chemical Engineering Science,* Volume 123, pp. 57-69.

Pani, F. et al., 1997. Kinetics of absorption of CO2 in concentrated aqueous methyldiethanolamine solutions in the range 296 K to 343 K. *Journal of Chemical & Engineering Data,* 42(2), pp. 353-359.

Penders-van Elk, N. J., Oversteegen, S. M. & Versteeg, G. F., 2016. Combined effect of temperature and p K a on the kinetics of absorption of carbon dioxide in aqueous alkanolamine and carbonate solutions with carbonic anhydrase. *Industrial & Engineering Chemistry Research,* 55(38), pp. 10044-10054.

Pinsent, B. R., Pearson, L. & Roughton, F. J., 1956. The kinetics of combination of carbon dioxide with hydroxide ions. *Transactions of the Faraday Society,* Volume 52, pp. 1512-1520.

Pohorecki, R. & Moniuk, W., 1988. Kinetics of reaction between carbon dioxide and hydroxyl ions in aqueous electrolyte solutions. *Chemical Engineering Science,* 43(7), pp. 1677-1684.

Prausnitz, J. M., Lichtenthaler, R. N. & De Azevedo, E. G., 1998. *Molecular thermodynamics of fluid-phase equilibria.* s.l.:Pearson Education.

Rinker, E. B., Sami, S. A. & Sandall, O. C., 1995. Kinetics and modelling of carbon dioxide absorption into aqueous solutions of N-methyldiethanolamine. *Chemical Engineering Science,* 50(5), pp. 755-768.

Rozanska, X., Wimmer, E. & de Meyer, F., 2021. Quantitative Kinetic Model of CO2 Absorption in Aqueous Tertiary Amine Solvents. *Journal of Chemical Information and Modeling,* 61(4), pp. 1814-1824.

Servia, A. et al., 2014. Modeling of the CO2 absorption in a wetted Wall column by piperazine solutions. *Oil & Gas Science and Technology-Revue d'IFP Energies nouvelles,* 69(5), pp. 885-902.

Sheng, M. et al., 2019. Effective Mass Transfer Area Measurement Using a CO2–NaOH System: Impact of Different Sources of Kinetics Models and Physical Properties. *Industrial & Engineering Chemistry Research,* 58(25), pp. 11082-11092.

Taylor, R. & Krishna, R., 1993. *Multicomponent mass transfer.* s.l.:John Wiley & Sons.

Thee, H. et al., 2012. Carbon dioxide absorption into unpromoted and borate-catalyzed potassium carbonate solutions. *Chemical Engineering Journal,* Volume 181–182, pp. 694-701.

Thomas, C., Loodts, V., Rongy, L. & De Wit, A., 2016. Convective dissolution of CO2 in reactive alkaline solutions: Active role of spectator ions. *International Journal of Greenhouse Gas Control,* Volume 53, pp. 230-242.

Versteeg, G. F., Kuipers, J. A., Van Beckum, F. P. & Van Swaaij, W. P., 1989. Mass transfer with complex reversible chemical reactions-I. Single reversible chemical reaction. *Chemical Engineering Science,* 44(10), pp. 2295-2310.

Versteeg, G. F. & Van Swaaij, W. P., 1988. Solubility and diffusivity of acid gases (carbon dioxide, nitrous oxide) in aqueous alkanolamine solutions. *Journal of Chemical & Engineering Data,* 33(1), pp. 29-34.

Weisenberger, S. & Schumpe, D. A., 1996. Estimation of gas solubilities in salt solutions at temperatures from 273 K to 363 K. *AIChE Journal,* 42(1), pp. 298-300.

Whitman, W. G., 1923. The two-film theory of gas absorption. *Chemical & Mellaurgy Engineering,* Volume 29, pp. 146-148.